Image Processing II

Chapter 9
Image reconstruction in the continuum

Prof. Michael Unser, LIB

April 2024

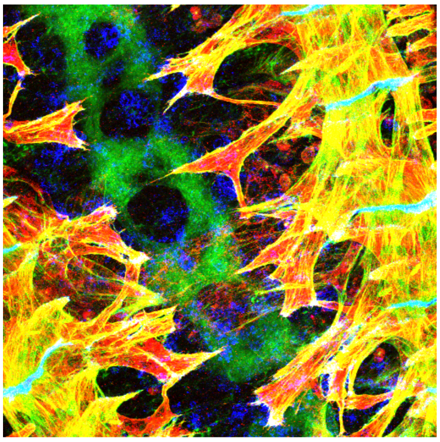

Measurement system

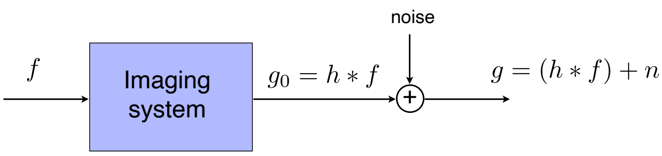

- Asumption of linearity and shift-invariance

$$g(\boldsymbol{x}) = (h * f)(\boldsymbol{x}) + n(\boldsymbol{x})$$

$$H(\boldsymbol{\omega}) = \mathcal{F}\{h\}(\boldsymbol{\omega}) = \int_{\mathbb{R}^d} h(\boldsymbol{x}) e^{-j\langle \boldsymbol{\omega}, \boldsymbol{x} \rangle} \mathrm{d}x_1 \cdots \mathrm{d}x_d \qquad \text{(optical transfer function)}$$

- Noise
  - Sources: counting statistics (shot noise), dark current (thermal noise), charge-to-voltage conversion errors (CCD read-out noise)
  - Statistical distribution: white Gaussian, Poisson (fluorescence, confocal microscopy), or speckle (ultrasound, coherent imaging)

Deconvolution challenge

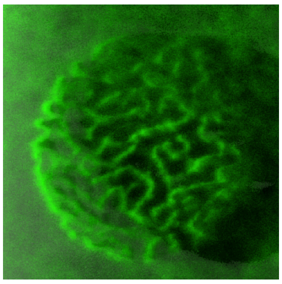

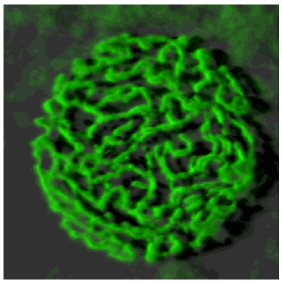

Original 3D data

Max. likelihood deconv (30 iterations)
(Huygens software)

DNA in the nucleus of a sea-urchin cell. The images are of size 512 x 512 x 80

TABLE OF CONTENT

9.1 DECONVOLUTION BY LSI FILTERING

- Restoration algorithm: linear, space-invariant filter

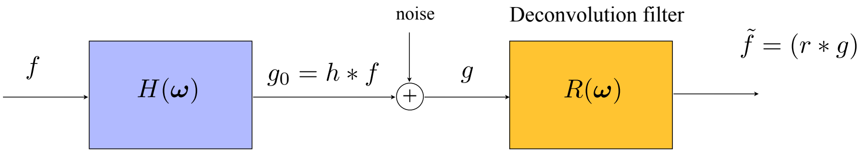

$$G_0(\omega) = H(\omega) \cdot F(\omega)$$

$$\begin{aligned}\tilde{F}(\omega) &= R(\omega) \cdot G(\omega) \\ &= \underbrace{R(\omega) \cdot G_0(\omega)}_{\text{signal contribution}} + \underbrace{R(\omega) \cdot N(\omega)}_{\text{noise contribution}}\end{aligned}$$

- Problems
  - How to select the optimal filter
  - How to balance signal recovery versus noise amplification

Restoration by inverse filtering

- Inverse-filtering solution

  Assumption: measurement noise is negligible

  $$G(\omega) \simeq H(\omega) \cdot F(\omega)$$

  $$\Rightarrow \quad R_{\text{inv}}(\omega) = \frac{1}{H(\omega)}$$

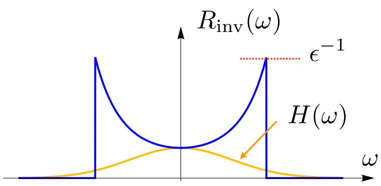

- Limitations
  - Inverse filter may be unstable

    $\Rightarrow$ stabilized version

    $$R_{\text{inv}}(\omega) = \begin{cases} \frac{1}{H(\omega)}, & |H(\omega)| \geqslant \epsilon > 0 \\ 0, & \text{otherwise} \end{cases}$$

  - Amplification of noise

    $$\tilde{F}(\omega) = R_{\text{inv}}(\omega) \cdot (G_0(\omega) + N(\omega)) = \underbrace{F(\omega)}_{\text{signal}} + \underbrace{R_{\text{inv}}(\omega) \cdot N(\omega)}_{\text{amplified noise}}$$

Inverse filtering (Cont'd)

- Blur (noise-free)

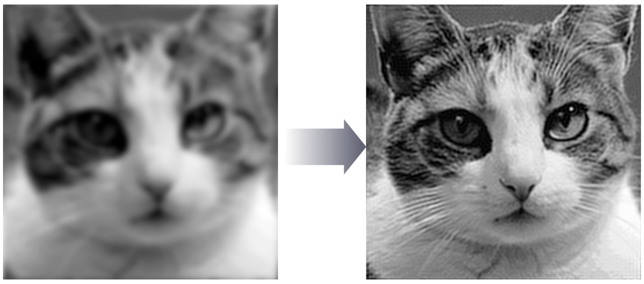

- Original image

Inverse filtering (stabilized version)

- Blur + additive noise

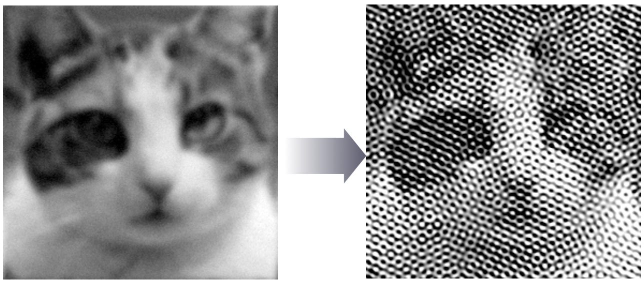

Wiener filter

- Basic hypothesis: $g = (h * f) + n$

  Signal f = realization of a wide-sense stationary process with known 2^{nd}-order statistics

  Spatial autocorrelation function: $E\{f(\boldsymbol{x})f(\boldsymbol{y})\} = c_f(\boldsymbol{x} - \boldsymbol{y})$

- A priori knowledge

  $H(\boldsymbol{\omega})$: optical transfer function

  $\Phi_f(\boldsymbol{\omega}) = \mathcal{F}\{c_f(\boldsymbol{x})\}(\boldsymbol{\omega})$: Power spectrum of signal

  $\Phi_n(\boldsymbol{\omega}) = \mathcal{F}\{c_n(\boldsymbol{x})\}(\boldsymbol{\omega})$: Power spectrum of noise; typ., $\Phi_n(\boldsymbol{\omega}) = \sigma^2$ (white noise)

- Optimal Wiener filter

  Minimum mean-square error (MMSE) estimator

$$R_{\mathrm{Wiener}}(\boldsymbol{\omega}) = \frac{\Phi_f(\boldsymbol{\omega})H^*(\boldsymbol{\omega})}{\Phi_f(\boldsymbol{\omega})|H(\boldsymbol{\omega})|^2 + \Phi_n(\boldsymbol{\omega})}$$

Wiener filter (Cont'd)

- Wiener filter: extreme cases

Noise is negligible	Noise is dominant
$\Phi_n(\boldsymbol{\omega}) \ll \Phi_f(\boldsymbol{\omega}) \cdot \lvert H(\boldsymbol{\omega})\rvert^2$ $\Downarrow$ $R_{\text{Wiener}}(\boldsymbol{\omega}) \approx \frac{1}{H(\boldsymbol{\omega})}$ (inverse filter)	$\Phi_n(\boldsymbol{\omega}) \gg \Phi_f(\boldsymbol{\omega}) \cdot \lvert H(\boldsymbol{\omega})\rvert^2$ $\Downarrow$ $R_{\text{Wiener}}(\boldsymbol{\omega}) \approx 0$ (suppression)

- Example

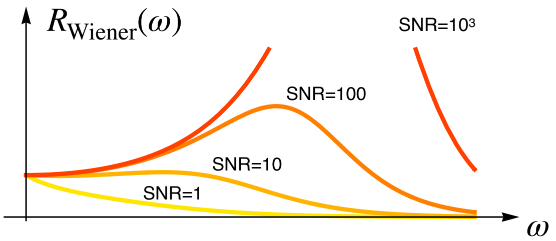

$H(\boldsymbol{\omega}) = e^{-\|\boldsymbol{\omega}\|^2/(2B^2)}$: Gaussian blur

$\Phi_f(\boldsymbol{\omega}) = \sigma_0^2 \cdot \|\boldsymbol{\omega}\|^{-\gamma}$: predominantly lowpass spectrum

$\Phi_n(\boldsymbol{\omega}) = \sigma^2$: White noise

$\text{SNR} = \sigma_0^2/\sigma^2$: quadratic signal-to-noise ratio

Derivation of the Wiener filter

Hypothesis: $\tilde{f} = r * \overbrace{(h * f + n)}^{g}$ where f and n are realizations of stationary processes

$$\text{MSE} = \mathbb{E}\{|\tilde{f} - f|^2\} = \mathbb{E}\{|\tilde{f}|^2\} - 2\,\mathbb{E}\{\tilde{f} \cdot f\} + \mathbb{E}\{|f|^2\}$$

Wiener-Khinchin theorem

$$\mathbb{E}\{|\tilde{f}|^2\} = \frac{1}{(2\pi)^d} \int_{\mathbb{R}^d} |R(\boldsymbol{\omega})|^2\, \Phi_g(\boldsymbol{\omega})\, \mathrm{d}\omega_1 \cdots \mathrm{d}\omega_d \qquad \Phi_g(\boldsymbol{\omega}) = |H(\boldsymbol{\omega})|^2 \Phi_f(\boldsymbol{\omega}) + \Phi_n(\boldsymbol{\omega})$$

$$\mathbb{E}\left\{|f|^2\right\} = \frac{1}{(2\pi)^d} \int_{\mathbb{R}^d} \Phi_f(\boldsymbol{\omega})\, \mathrm{d}\omega_1 \cdots \mathrm{d}\omega_d$$

$$\mathbb{E}\{\tilde{f} \cdot f\} = \text{Re}\left(\frac{1}{(2\pi)^d} \int_{\mathbb{R}^d} R^*(\boldsymbol{\omega}) H^*(\boldsymbol{\omega}) \Phi_f(\boldsymbol{\omega})\, \mathrm{d}\omega_1 \cdots \mathrm{d}\omega_d\right) \qquad \text{(hyp: } \Phi_{fn}(\boldsymbol{\omega}) = 0)$$

$$\Rightarrow \quad \text{MSE} = \frac{1}{(2\pi)^d} \int_{\mathbb{R}^d} |R(\boldsymbol{\omega})|^2 \Phi_g(\boldsymbol{\omega}) - 2\text{Re}\big(R^*(\boldsymbol{\omega}) H^*(\boldsymbol{\omega}) \Phi_f(\boldsymbol{\omega})\big) + \Phi_f(\boldsymbol{\omega})\, \mathrm{d}\omega_1 \cdots \mathrm{d}\omega_d$$

$$= \frac{1}{(2\pi)^d} \int_{\mathbb{R}^d} \left(\Phi_g(\boldsymbol{\omega}) \left| R(\boldsymbol{\omega}) - \frac{H^*(\boldsymbol{\omega}) \Phi_f(\boldsymbol{\omega})}{\Phi_g(\boldsymbol{\omega})} \right|^2 - \frac{|H(\boldsymbol{\omega})|^2 |\Phi_f(\boldsymbol{\omega})|^2}{\Phi_g(\boldsymbol{\omega})} + \Phi_f(\boldsymbol{\omega})\right) \mathrm{d}\omega_1 \cdots \mathrm{d}\omega_d$$

Since $\Phi_g(\boldsymbol{\omega}) \geqslant 0, \quad \forall \boldsymbol{\omega} \in \mathbb{R}^d$

$$\text{MSE minimum when} \quad R(\boldsymbol{\omega}) - \frac{H^*(\boldsymbol{\omega}) \Phi_f(\boldsymbol{\omega})}{\Phi_f(\boldsymbol{\omega}) |H(\boldsymbol{\omega})|^2 + \Phi_n(\boldsymbol{\omega})} = 0$$

Wiener filter: properties

- Factorization: MMSE denoising of g followed by inverse filtering

$$R_{\text{Wiener}}(\boldsymbol{\omega}) = \frac{\Phi_f(\boldsymbol{\omega})\,|H(\boldsymbol{\omega})|^2}{\Phi_f(\boldsymbol{\omega})\,|H(\boldsymbol{\omega})|^2 + \Phi_n(\boldsymbol{\omega})} \cdot \frac{1}{H(\boldsymbol{\omega})} = \frac{\Phi_{h*f}(\boldsymbol{\omega})}{\Phi_{h*f}(\boldsymbol{\omega}) + \Phi_n(\boldsymbol{\omega})} \cdot \frac{1}{H(\boldsymbol{\omega})}$$

- Optimality properties
  - MMSE space-invariant restoration filter
  - MMSE linear estimator for stationary processes
  - MMSE estimator for Gaussian stationary processes

- Limitations
  - Spectral power densities are not always known
  - Can be outperformed by space-variant and/or nonlinear algorithms

9.2 RADON TRANSFORM AND FILTERED BACKPROJECTION

- Radon transform
- Sinogram
- Backprojection
- Inverse Radon transform
- Filtered backprojection
- Sampling considerations

Projection and Radon transform

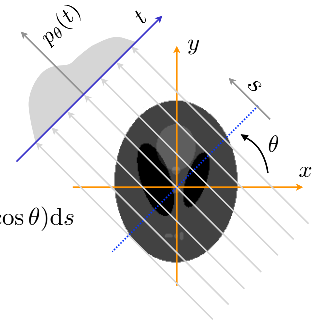

Johann Radon 1887-1956

$$\begin{pmatrix} x \\ y \end{pmatrix} = \begin{bmatrix} \cos\theta & -\sin\theta \\ \sin\theta & \cos\theta \end{bmatrix} \begin{pmatrix} t \\ s \end{pmatrix}$$
$$\Updownarrow$$
$$\begin{pmatrix} t \\ s \end{pmatrix} = \begin{bmatrix} \cos\theta & \sin\theta \\ -\sin\theta & \cos\theta \end{bmatrix} \begin{pmatrix} x \\ y \end{pmatrix}$$

- Radon transform

$$\mathcal{R} : L_1(\mathbb{R}^2) \quad \to \quad L_1(\mathbb{R} \times [0,\pi])$$

$$p_\theta(t) = \mathcal{R}\{f\}(t,\theta) = \int_{\mathbb{R}} f(t\cos\theta - s\sin\theta,\ t\sin\theta + s\cos\theta)\mathrm{d}s$$
$$= \int_{\mathbb{R}^2} f(\boldsymbol{x})\,\delta(t - \boldsymbol{\theta}^\mathsf{T}\boldsymbol{x})\mathrm{d}x\mathrm{d}y$$

Unit vector along t-axis: $\boldsymbol{\theta} = (\cos\theta, \sin\theta) \quad \Rightarrow \quad t = \boldsymbol{\theta}^\mathsf{T}\boldsymbol{x}$

> Boundedness: $f \in L_1(\mathbb{R}^2) \quad \Rightarrow \quad p_\theta = \mathrm{R}\{f\}(\cdot,\theta) \in L_1(\mathbb{R})$ for all $\theta \in [0,\pi]$
> $\Rightarrow \quad \|\mathrm{R}\{f\}(\cdot,\theta)\|_{L_1(\mathbb{R}\times[0,\pi])} = \int_0^\pi \int_{\mathbb{R}} |\mathrm{R}\{f\}(t,\theta)|\mathrm{d}t\mathrm{d}\theta \le \pi\|f\|_{L_1(\mathbb{R}^2)}$

- Sinogram

Trajectory of a point (x_0, y_0) in Radon space:

$$t_0(\theta) = x_0\cos\theta + y_0\sin\theta \qquad \Leftrightarrow \qquad t_0 = \boldsymbol{\theta}^\mathsf{T}\boldsymbol{x}_0$$

In polar coordinates: $x_0 = r\cos\phi,\quad y_0 = r\sin\phi \qquad \Rightarrow \quad t_0 = r\cos(\theta - \phi)$

Sinograms

$$\mathcal{R}\{f\}(t,\theta) = p_\theta(t)$$

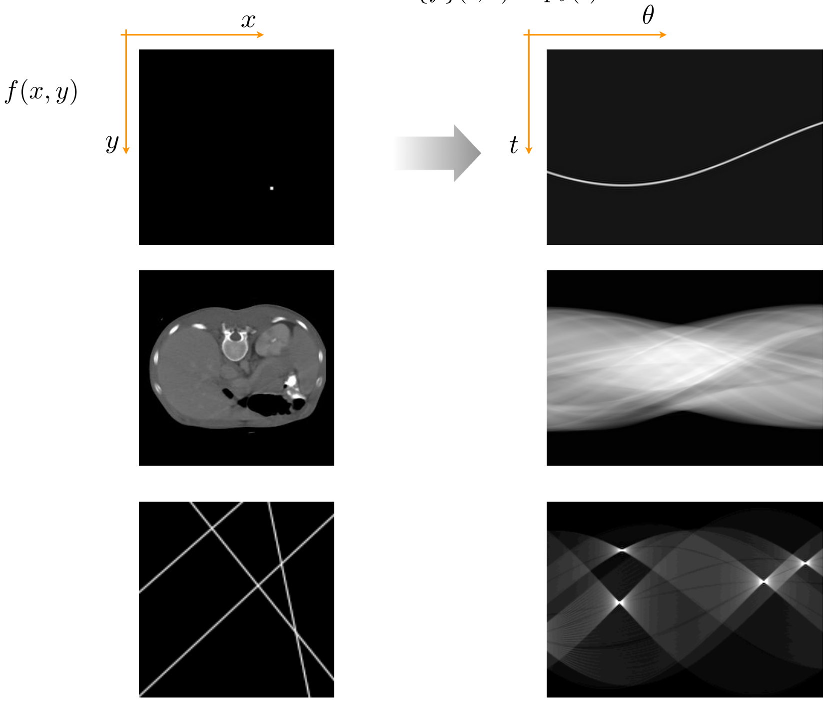

Fourier slice with $\boldsymbol{\omega} = \omega\boldsymbol{\theta}$:
$\mathcal{F}\{\delta(\cdot - \boldsymbol{x}_0)\}(\boldsymbol{\omega}) = \mathrm{e}^{-\mathrm{j}\langle\boldsymbol{\omega},\boldsymbol{x}_0\rangle} = \mathrm{e}^{-\mathrm{j}\omega\langle\boldsymbol{\theta},\boldsymbol{x}_0\rangle}$

Properties of the Radon transform

Context: $f \in L_1(\mathbb{R}^2) \quad \Rightarrow \quad \hat{f} = \mathcal{F}\{f\} \in C_0(\mathbb{R}^2)$ (i.e., $\hat{f}(\boldsymbol{\omega})$ is bounded and continuous)

Polar representation of Fourier transform:

$$\hat{f}_{\mathrm{pol}}(\omega, \theta) = \hat{f}(\boldsymbol{\omega})\big|_{\boldsymbol{\omega}=(\omega\cos\theta,\ \omega\sin\theta)} \quad \text{where} \quad \hat{f}(\boldsymbol{\omega}) = \int_{\mathbb{R}^2} f(\boldsymbol{x})\mathrm{e}^{-\mathrm{j}\langle\boldsymbol{\omega},\boldsymbol{x}\rangle}\mathrm{d}\boldsymbol{x}$$

- Fourier-slice theorem: $\displaystyle\int_{\mathbb{R}} \mathcal{R}\{\varphi\}(t,\theta)\mathrm{e}^{-\mathrm{j}\omega t}\mathrm{d}t = \hat{\varphi}(\boldsymbol{\omega})|_{\boldsymbol{\omega}=\omega\boldsymbol{\theta}}$

$p_\theta(t) = \mathcal{R}\{\varphi\}(t,\theta)$ (projection at angle θ)

$\hat{p}_\theta(\omega) = \hat{\varphi}(\omega\cos\theta, \omega\sin\theta)$

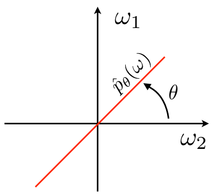

- Projected translation invariance: $\mathrm{R}\{\varphi(\cdot - \boldsymbol{x}_0)\}(t,\theta) = \mathrm{R}\{\varphi\}(t - \langle\boldsymbol{\theta}, \boldsymbol{x}_0\rangle, \theta)$

  Justification: Fourier-slice Theorem + phase shift with $\mathrm{e}^{-\mathrm{j}\langle\boldsymbol{\omega},\boldsymbol{x}_0\rangle} = \mathrm{e}^{-\mathrm{j}\omega\langle\boldsymbol{\theta},\boldsymbol{x}_0\rangle}$

- Pseudo-distributivity with respect to convolution

  For any fixed θ : $\mathrm{R}\{\varphi * \phi\}(t,\theta) = (p_\theta * q_\theta)(t)$ where $p_\theta(t) = \mathrm{R}\{\varphi\}(t,\theta)$ and $q_\theta(t) = \mathrm{R}\{\phi\}(t,\theta)$

Backprojection

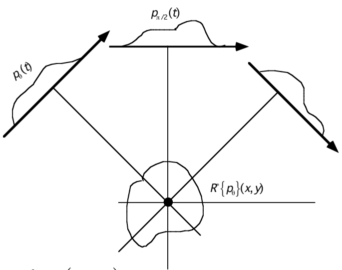

- Backprojection operator

  $\mathcal{R}^*: \quad L_\infty(\mathbb{R}\times[0,\pi]) \to L_\infty(\mathbb{R}^2)$

  $$b(x,y) = \mathcal{R}^*\{p_\theta(t)\}(x,y) = \int_0^\pi p_\theta(x\cos\theta + y\sin\theta)\,\mathrm{d}\theta$$

  Interpretation: accumulation of the ray-sums of all rays passing through the point (x,y)

- Adjoint property

  The backprojection is the adjoint of the projection operator $\mathcal{R}$

  $$\forall f \in L_1(\mathbb{R}^2),\ \forall p \in L_\infty(\mathbb{R}\times[0,\pi]), \quad \langle\mathcal{R}f, p\rangle_{\mathrm{Rad}} = \langle f, \mathcal{R}^* p\rangle$$

Duality products:

$\forall(f,g) \in L_1(\mathbb{R}^2)\times L_\infty(\mathbb{R}^2): \quad \langle f,g\rangle \triangleq \int_{\mathbb{R}^2} f(x,y)g(x,y)\mathrm{d}x\mathrm{d}y$

$\forall(p,q) \in L_1(\mathbb{R}\times[0,\pi])\times L_\infty(\mathbb{R}\times[0,\pi]): \quad \langle p,q\rangle_{\mathrm{Rad}} \triangleq \int_0^\pi\int_{\mathbb{R}} p_\theta(t)q_\theta(t,\theta)\mathrm{d}t\mathrm{d}\theta$

  Interpretation

  - $\mathcal{R}^*$ is the flow-graph transpose of $\mathcal{R}$
  - If $\mathcal{R}$ is represented by a matrix $\mathbf{R}$, then its adjoint is $\mathbf{R}^{\mathsf{T}}$

    $$\langle\mathbf{u}, \mathbf{R}\mathbf{v}\rangle = \mathbf{u}^{\mathsf{T}}\mathbf{R}\mathbf{v} = \left(\mathbf{R}^{\mathsf{T}}\mathbf{u}\right)^{\mathsf{T}}\mathbf{v} = \langle\mathbf{R}^{\mathsf{T}}\mathbf{u}, \mathbf{v}\rangle$$

Reconstruction by backprojection

- Approximate reconstruction

$$g(x,y) = \mathcal{R}^*\{p_\theta(t)\}(x,y) = \mathcal{R}^*\mathcal{R}\{f\}(x,y)$$

You don't know where the contribution comes from; thus, you put it back everywhere!

$\Rightarrow$ Blurring effect!

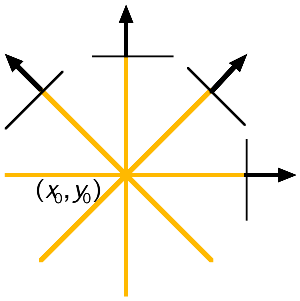

- Impulse response

$$\mathcal{R}^*\mathcal{R}\{\delta\}(x,y) = \frac{1}{\sqrt{x^2+y^2}} = \frac{1}{\|\boldsymbol{x}\|} \quad \stackrel{\mathcal{F}}{\longleftrightarrow} \quad \frac{2\pi}{\|\boldsymbol{\omega}\|} \quad \text{(isotropic)}$$

- Linear shift-invariant system

$$\mathcal{R}^*\mathcal{R}\{f\}(x,y) = \left(f * \frac{1}{\|\cdot\|}\right)(x,y)$$

Determination of impulse response

- Projection of an impulse

$$\mathcal{R}\{\delta(\cdot - x_0, \cdot - y_0)\}(x,y) = \delta(t - x_0\cos\theta - y_0\sin\theta) \qquad \text{(sinogram)}$$

- Backprojection of the impulse

$$\delta_\theta(t) = \delta(t - x_0\cos\theta - y_0\sin\theta)$$

$$\mathcal{R}^*\{\delta_\theta\}(x,y) = \int_0^\pi \delta(x\cos\theta + y\sin\theta - x_0\cos\theta - y_0\sin\theta)\,\mathrm{d}\theta$$

$$\mathcal{R}^*\{\delta_\theta\}(x,y) = \int_0^\pi \delta((x-x_0)\cos\theta + (y-y_0)\sin\theta)\,\mathrm{d}\theta = \frac{1}{\sqrt{(x-x_0)^2+(y-y_0)^2}}$$

Let $g(t)$ be such that $g(t_n) = 0$.
Then, $\delta(g(t)) = \sum_n \frac{\delta(t-t_n)}{g'(t_n)}$

Hint: Make change of variable $\theta = \arctan(t)$

$\Rightarrow \quad \cos(\theta) = \frac{\mathrm{sign}(t)}{\sqrt{1+t^2}}, \quad \sin(\theta) = \frac{|t|}{\sqrt{1+t^2}}, \quad \mathrm{d}\theta = \frac{\mathrm{d}t}{1+t^2}$

$\Rightarrow \quad \mathcal{R}^*\{\delta_\theta\}(x,y) = \int_{-\infty}^{\infty} \delta((x-x_0) + t(y-y_0))\frac{\mathrm{d}t}{\sqrt{1+t^2}}$

Backprojection at work

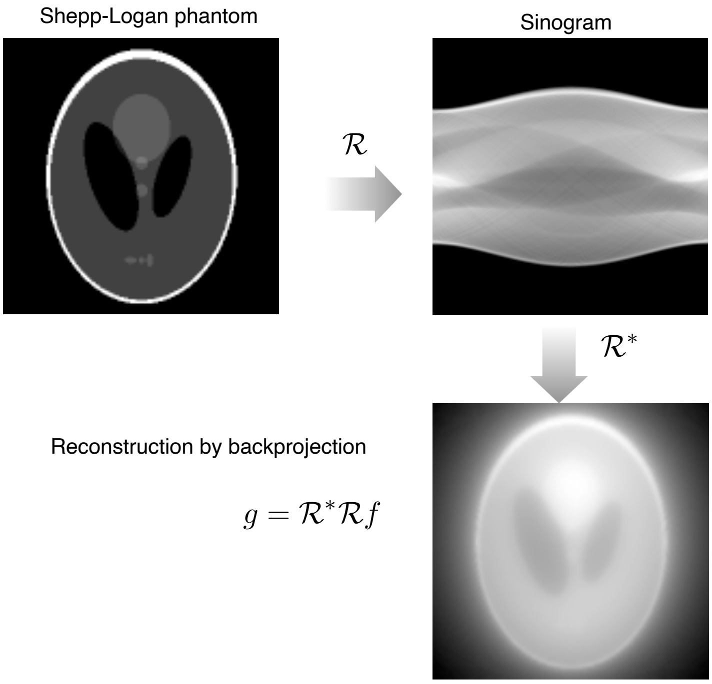

Inverse Radon transform

Hypothesis: $f \in L_1(\mathbb{R}^2) \quad \Rightarrow \quad \hat{f} = \mathcal{F}\{f\} \in C_0(\mathbb{R}^2)$ and $\mathrm{R}\{f\} \in L_1(\mathbb{R} \times [0, \pi])$

- Central-slice theorem: $\hat{p}_\theta(\omega) = \hat{f}(\omega \cos\theta, \, \omega \sin\theta) = \hat{f}_{\mathrm{pol}}(\omega, \theta)$
- Fourier-based reconstruction: $f(\boldsymbol{x}) = \dfrac{1}{(2\pi)^2} \displaystyle\int_{\mathbb{R}^2} \hat{f}(\boldsymbol{\omega}) \mathrm{e}^{\mathrm{j}\langle \boldsymbol{\omega}, \boldsymbol{x} \rangle} \, \mathrm{d}\omega_x \mathrm{d}\omega_y$
- Reconstruction by filtered backprojection: $f(x, y) = \mathcal{R}^*\{q_\theta(t)\}(x, y)$

  where $q_\theta(t) = (h * p_\theta)(t)$ with $h(t) \overset{\mathcal{F}}{\longleftrightarrow} \dfrac{|\omega|}{2\pi}$

Proof: Fourier reconstruction in polar coordinates

$$f(x, y) = \frac{1}{(2\pi)^2} \int_0^{2\pi} \int_0^{+\infty} \underbrace{\hat{f}_{\mathrm{pol}}(\omega, \theta)}_{\hat{p}_\theta(\omega)} \mathrm{e}^{\mathrm{j}\omega t} \, |\omega| \, \mathrm{d}\omega \mathrm{d}\theta \qquad \text{with} \quad t = x\cos\theta + y\sin\theta$$

Central-slice theorem + Fourier symmetry: $\hat{f}_{\mathrm{pol}}(\omega, \theta + \pi) = \hat{f}_{\mathrm{pol}}(-\omega, \theta) = \hat{p}_\theta(-\omega)$

$$\Rightarrow \quad f(x, y) = \int_0^{\pi} \underbrace{\frac{1}{2\pi} \left(\int_{-\infty}^{+\infty} \hat{p}_\theta(\omega) \cdot \frac{|\omega|}{2\pi} \cdot \mathrm{e}^{\mathrm{j}\omega t} \, \mathrm{d}\omega \right)}_{q_\theta(t)} \mathrm{d}\theta$$

Filtered backprojection

- Theoretical formula: $f(x,y) = \mathcal{R}^*\{q_\theta(t)\}(x,y) = \int_0^\pi q_\theta(x\cos\theta + y\sin\theta)\,\mathrm{d}\theta$

  where $q_\theta(t) = (h * p_\theta)(t)$ and $h(t) \overset{\mathcal{F}}{\longleftrightarrow} \frac{|\omega|}{2\pi}$

- Discrete implementation
  - Discrete data $\Rightarrow$ Digital filtering & Interpolation
  - Finite number of projections $\Rightarrow$ Quadrature formula

- Discrete backprojection

  Loop over pixels: $\tilde{f}(x,y) = \underbrace{\left(\frac{\pi}{N}\right)}_{\Delta\theta} \cdot \sum_{i=1}^{N} q_{\theta_i}(x\cos\theta_i + y\sin\theta_i)$

  Use interpolation to evaluate $q_{\theta_i}(t)$ for t non-integer (piecewise-linear or higher-order spline)

FBP filters

- 1D Filtering step

  Loop over projections: $(p_{\theta_i}[k], i = 1, \ldots, N)$

  FFT: $p_{\theta_i}[k] \overset{\text{FFT}}{\longrightarrow} P_{\theta_i}(e^{jn\omega_0})$

  Filtering: $Q_{\theta_i}(e^{jn\omega_0}) = H(e^{jn\omega_0}) \cdot P_{\theta_i}(e^{jn\omega_0})$

  Inverse FFT: $Q_{\theta_i}(e^{jn\omega_0}) \overset{\text{FFT}^{-1}}{\longrightarrow} q_{\theta_i}[k]$

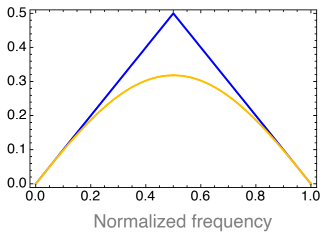

  - Ram-Lak filter [Ramachandran & Lakshminarayanan, 1971]

    $$\hat{h}_{\mathrm{RL}}(\omega) = \frac{|\omega|}{2\pi} \cdot \mathrm{rect}\left(\frac{\omega}{2\omega_{\max}}\right)$$

  - Shepp-Logan filter [Shepp & Logan, 1974]

    $$\hat{h}_{\mathrm{SL}}(\omega) = \frac{|\omega|}{2\pi} \cdot \mathrm{sinc}\left(\frac{\omega}{2\omega_{\max}}\right) \cdot \mathrm{rect}\left(\frac{\omega}{2\omega_{\max}}\right)$$

FBP at work

Shepp-Logan phantom

$$f = f(x, y)$$

$\mathcal{R}$ →

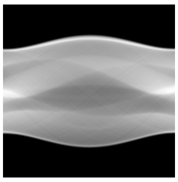

Sinogram

↓ $\mathcal{K} \overset{\mathcal{F}}{\longleftrightarrow} \dfrac{|\omega|}{2\pi}$

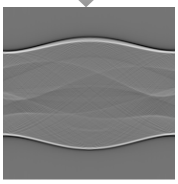

Filtered sinogram (Ram-Lak)

← $\mathcal{R}^*$

FBP reconstruction

$$f = \mathcal{R}^* \mathcal{K} \mathcal{R} f$$

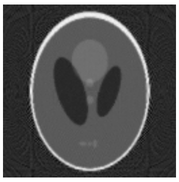

Backprojection only

$$g = \mathcal{R}^* \mathcal{R} f$$

FBP sampling considerations

- Hypotheses

  $\hat{f}_{\rm pol}(\omega, \theta)$ is *essentially bandlimited* to $\omega_{\max}$

  $f_{\rm pol}(r, \phi)$ is *essentially space-limited* to $R_{\max}$

- Maximum sampling step

  $$\boxed{\Delta x \leqslant \frac{\pi}{\omega_{\max}}}$$ (Shannon)

  $\Rightarrow \quad M_{\min} = \frac{2R_{\max}}{\Delta x}$ samples per view

- Minimum number of views

  $N_{\min} = \frac{\pi\omega_{\max}}{\Delta\omega} = \omega_{\max} R_{\max}$ [Brooks & Weiss, 1978]

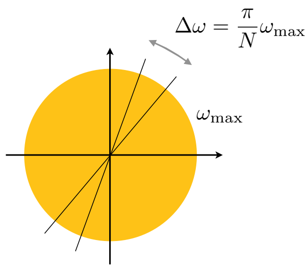

Maximum spectral sampling gap: $$\boxed{\Delta\omega \leqslant \frac{\pi}{R_{\max}}}$$ (Shannon in reverse)

Appendix A. X-ray computer (assisted) tomography (CT or CAT)

GODFREY N. HOUNSFIELD
Developed computer-assisted tomography.
Constructed first clinical CT-scan in 1972.
1979 Nobel Prize in medicine

ALAN M. CORMACK
Demonstrated the theoretical feasibility of X-ray computer-assisted tomography.
[model experiment in 1963-64]
1979 Nobel Price in medicine

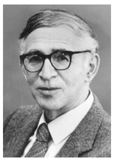

AARON KLUG
Developed computational techniques for the 3D reconstruction of electron micrographs.
[first 3D reconstruction in 1968]
1982 Nobel Prize in Chemistry

And a few other pioneers…

Physical principle: Absorption law

Interaction of EM radiation (X-rays or Gamma rays) with matter

$\Rightarrow$ Exponential law [Beer-Lambert]

μ: linear attenuation coefficient (cm^{-1})

- Homogeneous material

$$I = I_0 e^{-\mu w}$$

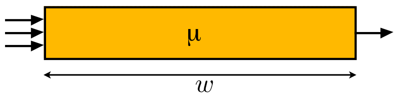

- Discrete components

$$I = I_0 \exp\left(-\sum_{i=1}^{n} \mu_i x_i\right)$$

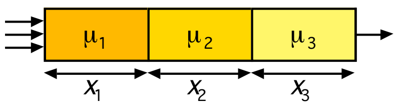

- Continuous medium

$$I = I_0 \exp\left(-\int_0^w \mu(x)\,\mathrm{d}x\right)$$

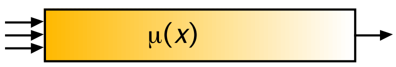

- Projection value

$$p = -\log\left(\frac{I}{I_0}\right) = \int_0^w \mu(x)\,\mathrm{d}x \quad \Rightarrow \text{ Line integral}$$

Computer-assisted tomography (CAT): measurement principle

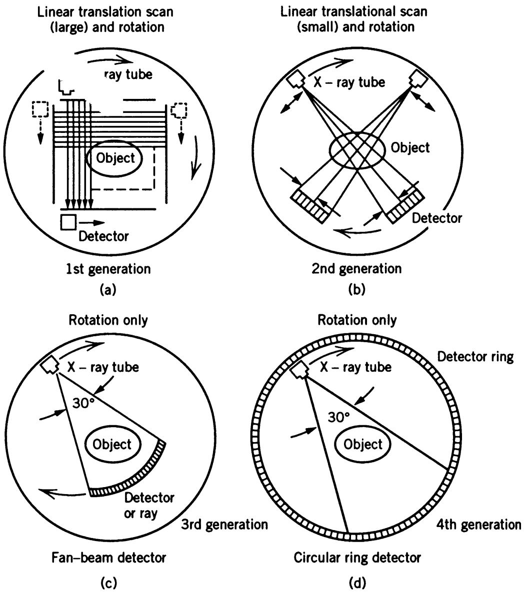

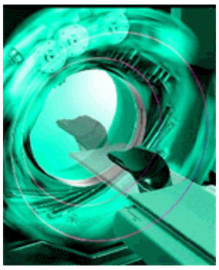

Modern X-ray scanner (GE)